5C.8 QUANTATIVE COMPARISON OF TRMM PRECIPITATION ALGORITHMS IN TROPICAL CYCLONES

Joseph P. Zagrodnik* and Haiyan Jiang
Florida International University, Miami, Florida

1. INTRODUCTION

Rainfall observations from the Tropical Rainfall Measuring Mission (TRMM) satellite have helped to quantify the total precipitation in tropical systems, initialize and validate numerical models, and decipher the relationship between Tropical Cyclone (TC) eyewall and rain band structure and intensity changes. However, these algorithms are calibrated on a global or regional scale and often show less agreement for smaller scale features such as TCs. The purpose of this study is to compare the properties of the Precipitation Radar (PR) 2A25 and TRMM Microwave Imager (TMI) 2A12 rainfall retrieval algorithms in TC inner cores and rainbands. The methodology does not involve a pixel-by-pixel comparison, but rather an evaluation of the rainfall distributions in the storm regions (inner cores and rainbands) as a whole. TC rainfall structure is highly variable on spatial and temporal scales and is related to the same environmental factors that contribute to intensification and weakening such as sea surface temperature (SST), vertical wind shear, and convective intensity. By comparing the algorithms on a storm region-size scale, it is easier to relate TC rainfall properties to these same environmental factors and to better understand TC rainfall structure for both algorithms.

2. DATA

The data for this study are derived from the TRMM Tropical Cyclone Precipitation Feature (TCPF) database (Jiang et al. 2011). The time frame spans 12 years from Dec. 1997-Dec. 2009, consisting of 13,677 individual TRMM overpasses of 1,013 TCs. Two precipitation retrieval algorithms are considered: Version 6 of the PR 2A25 algorithm (Iguchi et al. 2000) and the TMI 2A12 algorithm (Kummerow et al. 1996, 2001). The PR 2A25 has a pixel size of 5 x 5 km (4 x 4 km before 2001 orbital boost) compared with 8 x 6 km (7 x 5 km before boost) for the TMI 2A12. To stay within the range of both the PR and TMI, the study is limited to the Precipitation Radar's 247-km orbital swath (215 km before boost).

Region	Mean Radius (km)	Min Radius (km)	Max Radius (km)	Std. Dev.
IC	87	50	170	18
IB	163	90	270	28
OB	506	300	900	123

Table 1: Mean, minimum, maximum, and standard deviation of the outer edge of storm region separation radii.

Each individual overpass was subjectively classified into three sub-regions for detailed study by Ellen Ramirez (Cecil et al. 2002; Jiang and Ramirez 2011). The inner core (IC) region includes the eyewall and all near-center convection in storms without eyewalls. The inner rainband (IB) region includes banded or blob-like precipitation immediately outside the IC boundary. The outer rainband (OB) includes outward spiraling rainbands and all outlying TC-related features. Each storm is assigned an IC, IB, and OB radius which represent the outer edge of the respective storm regions. Compared with a fixed 100-km radius, this method accounts for varying TC size and reduces the contamination between the IC and IB regions. To remove samples that only capture a small portion of the storm region, minimum PR 2A25 raining area criteria of 5,000 km^2 are also set for each individual region. Table

* *Corresponding author address*: Joseph P. Zagrodnik, Florida International University, Dept. of Earth & Environment, Miami, Florida. Email: jzagr001@fiu.edu

1 displays the characteristics of the storm region separation radii.

3. RAIN RATE COMPARISONS

Statistical comparison of mean rain rate (mm hr^{-1}) between the two algorithms is conducted by calculating the mean values, histograms, and scatterplots for the three storm regions and four intensity categories.

3.1 *Mean Rain Rates*

Figure 1 displays the mean rain rate for IC, IB, and OB regions from storms of various intensities for the (a) PR 2A25 and (b) TMI 2A12. The PR 2A25 produces larger rain rates than the TMI 2A12 in all storm regions and intensities, with the difference always increasing with greater storm intensity. In the IB and OB regions, the greatest differences occur in storms of at least hurricane intensity. Overall, the algorithm difference is largest in the IC, especially hurricanes, where the mean PR 2A25 rain rate is about twice as high as the TMI 2A12. These are significant differences, especially considering they are averaged over the entire inner core.

3.2 *Rain Rate Histograms*

The histograms for rain rate for the IC, IB, and OB are displayed in Figure 2 (a-c). The IC distributions show high variability between algorithms and intensity categories. The algorithms are in best agreement for TDs and farthest apart for major hurricanes. The TMI 2A12 shows bell-shaped distributions which have a higher mode and widen slightly as intensity increases. The PR 2A25 has broader distributions that are highly skewed toward high rain rates. The histograms for hurricanes are of most interest due to the significant disagreement between algorithms. The TMI 2A12 has no cases with a rain rate greater than 15 mm hr^{-1}, while the PR 2A25 detects many more inner cores with rain rates in the 15-40 mm hr^{-1} range. For instance, the PR 2A25 estimates 38% of Cat. 3-5 hurricane IC cases with a rain rate greater than 20 mm hr^{-1} and none for the TMI 2A12. For Category 1-2 hurricanes, the PR 2A25 finds 21% of cases with a rain rate greater than 15 mm hr^{-1} and not a single case for the TMI 2A12. The TMI 2A12 places the majority of hurricane ICs in the 5-15 mm hr^{-1} range. In the IB and OB, rain rates still skew toward stronger intensities, but the spread is less than the IC.

3.3 *Rain Rate Scatterplots*

The scatterplot for IC rain rate (Fig. 2d) shows a strong bias toward higher PR 2A25 rain rates, especially for intense storms. The majority of Category 3-5 ICs have a higher PR 2A25 rain rate by a significant margin. In the most extreme

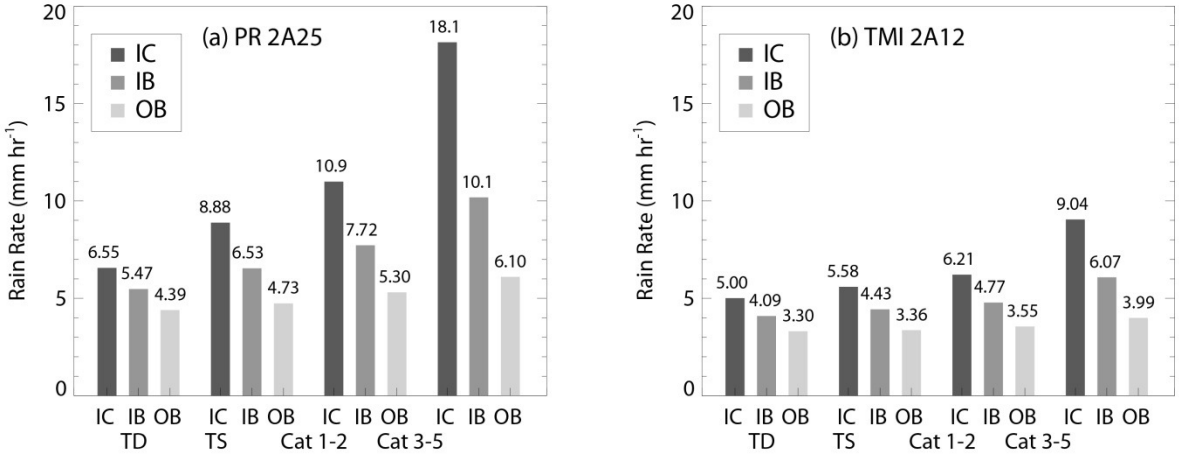

Figure 1: Bar plots comparing (a) PR 2A25 and (b) 2A12 mean rain rate for Inner Cores (dark shade), Inner Bands (medium shade), and Outer Bands (light shade), divided by storm intensity.

cases, the IC rain rate is 20-30 mm hr^{-1} greater than the TMI 2A12. Still, many ICs including some hurricanes show very good agreement between the algorithms. In 40% of ICs, the algorithms are within 2 mm hr^{-1} of each other. The correlation coefficient is lower for hurricanes than for weaker storms. In the IB and OB, the correlations improve, but most regions still show higher PR 2A25 rain rates.

4. DISCUSSION AND RELATION TO CONVECTIVE PARAMETERS

The difference between the algorithms (PR 2A25 minus TMI 2A12) is most closely correlated with the aerial coverage of heavy rain, specifically the area of PR reflectivity greater than 40 dBZ. A scatterplot comparison is shown in Figure 3. Linear correlations are highest in hurricane inner cores and inner bands (≥ 0.80), although the outer band region has only slightly lower correlations. The large difference in the algorithms is mostly caused by the TMI significantly underestimating these areas of heavy rain. Weaker storms do not have as strong of a relationship between algorithm differences and heavy rain because most only have a small percentage (< 5%) of rain with a PR reflectivity higher than 40 dBZ. The aerial coverage of ice-scattering parameters (85 and 37 GHz PCT) does not correlate well with the rain rate difference. Therefore, the juxtaposition of heavy rain and low ice scattering is poorly measured by the TMI 2A12 algorithm.

In the IC, the TMI 2A12 rain rate retrievals are more closely correlated with the area of 85 GHz PCT < 225 K (relative to raining area). In the IB and OB, the rain rate correlates best with the area of 85 GHz PCT < 250 K. Weaker storms (tropical depressions and storms) have a higher correlation than hurricanes (0.75-0.85 vs. 0.50-0.65). The TMI 2A12 rain rate also correlates well with the aerial coverage of 37 GHz PCT < 275 K, especially in outer bands and weaker storms.

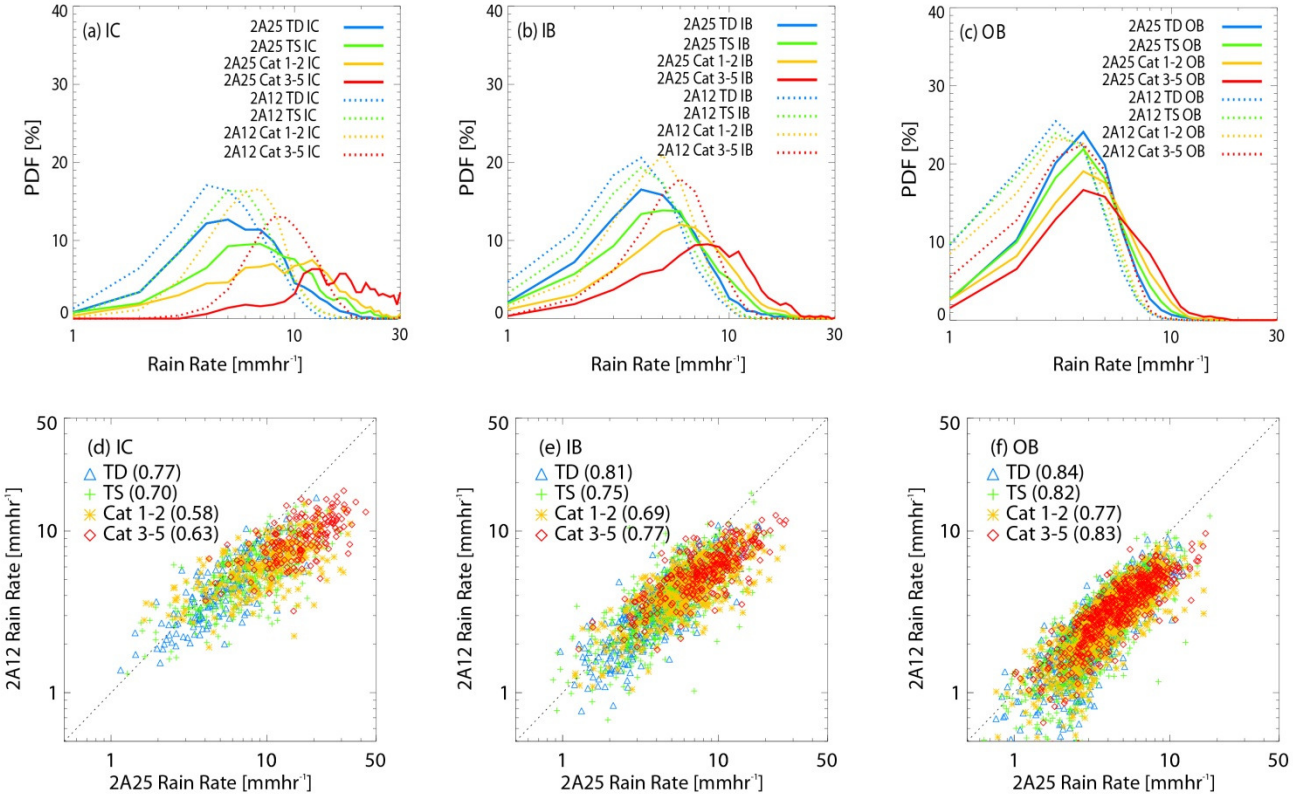

Figure 2: PDF of rain rate distributions for (a) IC, (b) IB, and (c) OB regions. Scatterplot of PR 2A25 (x-axis) vs. TMI 2A25 (y-axis) for (d) IC, (e) IB, and (f) OB regions. Linear correlation coefficients are in parentheses. All plots are color coded by storm intensity.

These convective parameters are good predictors of the mean 2A12 rain rate. However, an 85 GHz PCT of 225 K is typically associated with rain rates around 10-12 mm hr^{-1} (Mohr and Zipser 1996), which is less than the heavy rain rates that are most responsible for the algorithm differences. Lower 85 GHz PCT values (< 200 K) do not have a strong relation to the area of PR reflectivity > 40 dBZ, confirming that strong ice scattering is not a necessarily present above heavy rain. Future work will further investigate the spatial distribution of TC rainfall and convection using the Precipitation Radar.

5. ACKNOWLEDGEMENTS

This work was supported by NASA Headquarters under the NASA Earth and Space Science Fellowship Program – Grant "NNX11AP84H"

6. REFERENCES

Cecil, D.J., E.J. Zipser, and S.W. Nesbitt, 2002: Reflectivity, ice scattering, and lightning characteristics of hurricane eyewalls and rainbands. Part I: Quantitative description**.** *Mon Wea. Rev.,*130, 769-784.

Cecil, D. J. and M. Wingo, 2009: Comparison of TRMM rain-rate retrievals in tropical cyclones. *J. Meteor. Soc. Japan*, 87, 369-380.

Iguchi, T., T. Kozu, R. Meneghini, J. Awaka, K. Okamoto, 2000: Rain-Profiling Algorithm for the TRMM Precipitation Radar. *J. Appl. Meteor.*, 39, 2038–2052.

Jiang, H., C. Liu, E. J. Zipser, 2011: A TRMM-Based Tropical Cyclone Cloud and Precipitation Feature Database. *J. Appl. Meteor. Climatol.*,50, 1255–1274.

Jiang, H., 2011: The relationship between tropical cyclone intensity change and the strength of inner core convection. *Mon. Wea. Rev.*, **140**, 1164-1176.

Kummerow, C., W.S. Olson, and L.Giglio, 1996: Simplified Scheme for Obtaining Precipitation and Vertical Hydrometeor Profiles from passive Microwave Sensors. *IEEE Transactions on Geosci. and Remote Sensing.* 34, 1213-32.

Kummerow, C., and co-authors, 2001: The evolution of the Goddard Profiling Algorithm (GPROF) for rainfall estimation from passive microwave sensors. *J. Appl. Meteor.*, 40, 1801-1820.

Mohr, Karen I., Edward J. Zipser, 1996: Mesoscale Convective Systems Defined by Their 85-GHz Ice Scattering Signature: Size and Intensity Comparison over Tropical Oceans and Continents. *Mon. Wea. Rev.*, 124, 2417–2437.

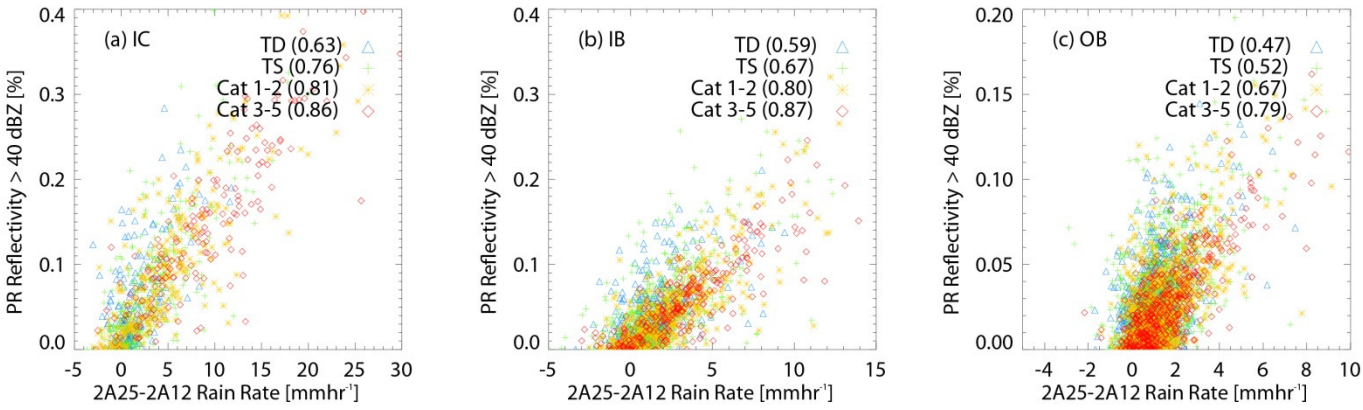

Figure 3: Scatterplots of the difference in PR and TMI rain rate (2A25 – 2A12) vs. percent coverage of PR reflectivity greater than 40 dBZ.